

# Hydroxyapatite and fluorapatite coatings on dental screws: effects of blast coating process and biological response

Conor F. Dunne · Barry Twomey · Ciara Kelly ·  
Jeremy C. Simpson · Kenneth T. Stanton

Received: 27 January 2014 / Accepted: 3 August 2014 / Published online: 13 January 2015  
© Springer Science+Business Media New York 2014

**Abstract** This paper describes the deposition of hydroxyapatite (HA) and fluorapatite (FA) onto titanium dental screws using a novel ambient temperature coating technique named CoBlast. The process utilises a coating medium and a blast medium sprayed simultaneously at the substrate surface. The blast medium was a sintered apatite (sHA) and two particles sizes ( $<106$  and  $<180$   $\mu\text{m}$ ) were used to assess their influence on the coating process. The influence of the coating process on the coating composition, coating adhesion, screw morphology and screw microstructure was examined. XRD analysis revealed the coating crystallinity was the same as the original HA and FA feedstock powders. Examining the screw's morphology, the threads of the CoBlasted screws exhibited rounding compared to the unmodified screw. This is due to the abrasive nature of the CoBlast process. The degree of rounding was more significant for the screws blasted with the 180  $\mu\text{m}$  sHA than the 106  $\mu\text{m}$  sHA. The blast media particle size significantly influences the surface roughness of both the substrate and coating and the microstructure of the substrate. The screws did not exhibit any loss of coating after insertion into a model bone material, indicating that the coating was strongly adhered to the substrate. There

was no statistically significant difference in cell attachment and cell morphology on the unmodified substrates compared to the coated substrates. In conclusion, the CoBlast process can be used to deposit HA and FA onto complex geometries such as dental screws. The choice of blast medium particle size influences the screws morphology. The coating process does not negatively impact on the cell attachment and morphology *in vitro*.

## 1 Introduction

Titanium and titanium alloys are commonly used in the fabrication of dental implants such as dental screws due to their light weight, high biocorrosion resistance, biocompatibility and mechanical properties [1]. Previous studies have shown that the long term clinical success of dental implants depends largely on the osteointegration of the implant [2]. Osteointegration is the formation of an interface between bone and the implant, without the presence of non-bone tissue between the bone and implant interface [3]. There are a number of factors that influence the rate of osteointegration such as surface roughness and surface chemistry [4–6].

Increasing the surface roughness of implants via grit-blasting, sand-blasting and acid etching has been shown to enhance the osteointegration of implants [7–9]. Surface roughness has been shown to influence cell attachment, proliferation and differentiation [10–12]. Grit blasted screws have been shown to exhibit a higher bone-to-metal contact than as-machined screws and require more torque to remove from bone than smooth screws [13–16]. The increase in surface roughness provides a greater surface area for mechanical interlock between the bone and the implant [17]. A range of surface roughness ( $R_a$ ) between

---

C. F. Dunne · K. T. Stanton (✉)  
UCD School of Mechanical and Materials Engineering,  
University College Dublin, Belfield, Dublin 4, Ireland  
e-mail: kenneth.stanton@ucd.ie

B. Twomey  
EnBio Ltd., NOVA UCD, Belfield Innovation Park, Dublin 4,  
Ireland

C. Kelly · J. C. Simpson  
UCD School of Biology and Environmental Science, University  
College Dublin, Belfield, Dublin 4, Ireland

1–10  $\mu\text{m}$  maximises the interlocking between the implant and the bone [3].

The osteointegration of an implant can be enhanced by altering the surface chemistry via the application of an osteoconductive coating. An osteoconductive surface is one that permits bone to grow on its surface or down into its pores by permitting cells to attach, proliferate and deposit bone matrix [4, 18]. The formation of bone on the surface of the implant is a prerequisite for osteointegration [4]. Hydroxyapatite (HA,  $\text{Ca}_{10}(\text{PO}_4)_6(\text{OH})_2$ ) [19, 20] is the most widely used osteoconductive coating for hard-tissue applications as it closely resembles the natural mineral phase of bone and teeth [21]. HA is biocompatible, biodegradable and osteoconductive [18]. In spite of their widespread use, HA coatings have been reported to be susceptible to delamination and dissolution and this can result in a loss of coating integrity and ultimately aseptic loosening of the implant [22–26]. To address this problem, other bioactive ceramics, such as fluorapatite (FA,  $\text{Ca}_{10}(\text{PO}_4)_6(\text{F})_2$ ), are being investigated as potential osteoconductive coatings [27].

Fluorapatite is analogous to HA. Like HA, FA is biocompatible, biodegradable and osteoconductive. However, FA has a number of advantages compared with HA: it is more chemically stable than HA due to its crystal structure. The  $\text{F}^-$  ions produce lower lattice strains than the  $\text{OH}^-$  ions in hydroxyapatite, this results in a more stable crystal structure [19]. The greater chemical stability of FA compared to HA results in a slower rate of degradation and this reduces the rate of coating resorption *in vivo* [28].

This paper investigates HA and FA coatings deposited on to dental screws using a novel coating technique, CoBlast<sup>TM</sup> [29–35]. CoBlast is an ambient temperature process developed to address the problems associated with high temperature coating techniques, such as the formation of unwanted phases, amorphization of the coating and poor adherence of the coating [23, 29, 30, 32, 34, 36–39]. The process utilises a co-incident stream of abrasive blast medium and a stream of coating medium particles to modify the substrate surface. The abrasive roughens the surface while simultaneously disrupting the passivating oxide layer of the substrate and exposing the reactive metal. The stream of dopant then reacts with the exposed reactive metal to form an intimate chemical bond [32]. The adhesion of the coating to the substrate is due to a combination of tribo-chemical bond formation and mechanical interlock between the bioceramic and the metal substrate [29].

Previous studies using the CoBlast process have deposited bioactive coatings onto flat metallic coupons. This paper investigates influence of this novel process on the deposition HA and FA onto more complex geometrical shapes (dental screws) and examines the influence of the

process on the coating adhesion, substrate microstructure, coating crystallinity and the biological response of the deposited coating *in vitro*.

## 2 Materials and methods

### 2.1 Materials

Five titanium (Grade 2) dental screws 8.5 mm in length with a maximum diameter of 3.75 mm were coated per set. Five titanium (Grade 2) 15 × 15 mm coupons of 1 mm thickness were coated per set. The titanium coupons were used in the surface characterisation of the coating and substrate using X-ray diffraction and surface roughness measurements. Hydroxyapatite (HA) and fluorapatite (FA) were used as the coating media. The HA (SAI, France) particle size used was 25–60  $\mu\text{m}$ . The FA (HIMED, U.S.A.) particle size was 5–30  $\mu\text{m}$ . A sintered apatite (sHA) (HIMED, U.S.A.) was used as the blast medium. Two particles sizes of sHA (<106, <180  $\mu\text{m}$ ) were used to assess the influence of the blast medium particle size on the screw morphology. Figure 1 shows SEM images of the coating media and abrasive blast media used in this study.

### 2.2 Sample preparation

The titanium screws and coupons were ultrasonically cleaned in 1 M HCl and then in isopropanol to remove any contaminants prior to surface modification. The titanium screws were rotated at 20 mm/min. The coating media (HA, FA) and blast medium (sHA) were sprayed simultaneously in the same stream through a single de Laval nozzle at the rotating titanium screws with a jet pressure of 80 psi, at a height of 50 mm from the screws with an axial travel speed of 13 mm/min. The duration of the coating process for each 8.5 mm long screw was 40 s.

The flat titanium coupons were placed on a stationary tray. The coating media (HA, FA) and blast medium (sHA) were sprayed at the stationary titanium coupons with a jet pressure of 80 psi, at a height of 50 mm from the substrate with a nozzle travel speed of 13 mm/min. And a raster offset of 4.5 mm. Figure 2 shows a schematic of the coating process. To act as a control for the cell studies, a duplicate set of samples coated with HA/180  $\mu\text{m}$  sHA were etched in 1 M HCl to remove the HA coating. This provided a rough surface without a bioactive coating for the *in vitro* studies.

### 2.3 Surface characterisation

X-ray diffraction was carried out on the titanium coupons using a Siemens D500 diffractometer with rotating stage and

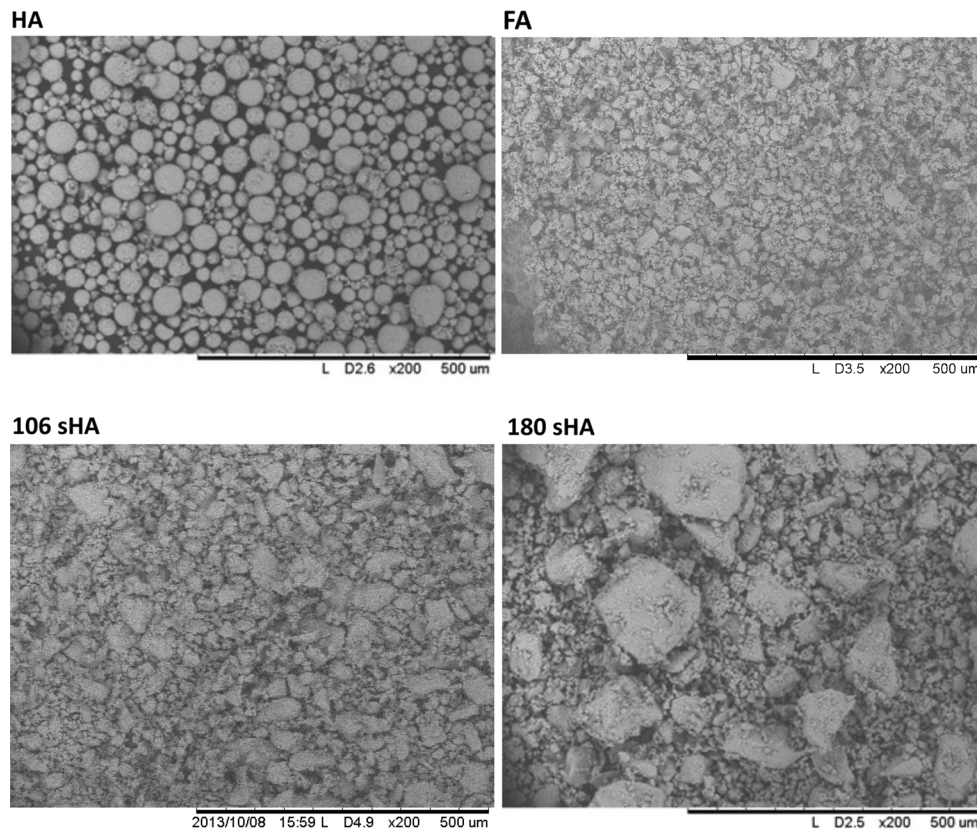


**Fig. 1** SEM images of HA, FA, <106 and <180 μm sHA powders

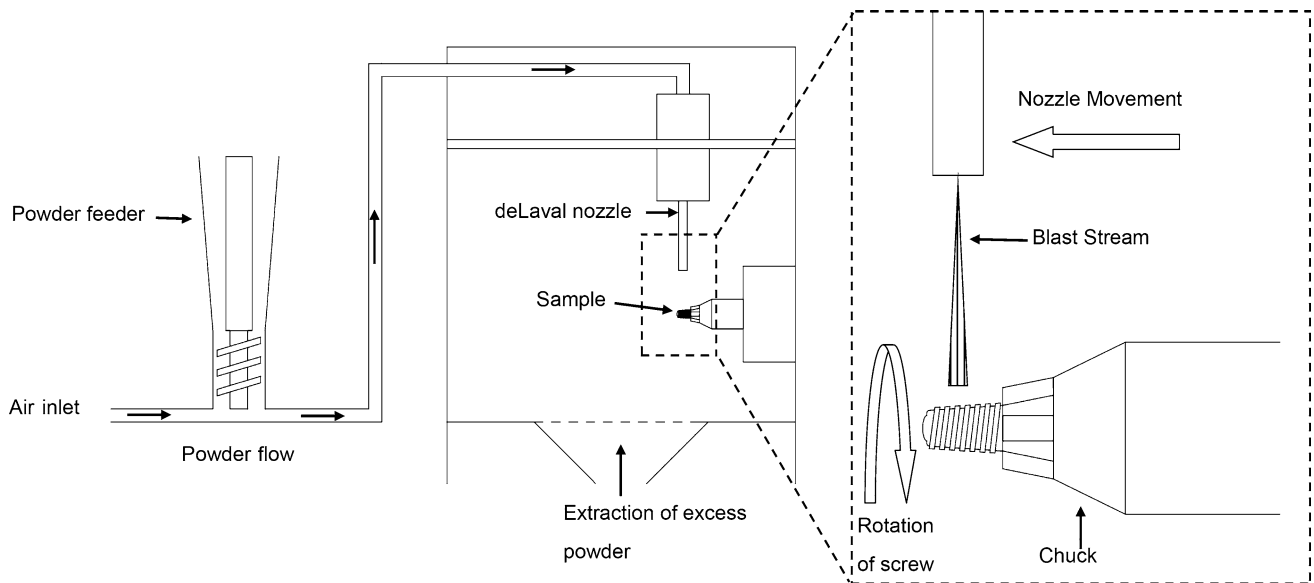


**Fig. 2** Schematic of surface modification process

beam monochromator (Cu K $\alpha$ ) (Munich, Germany). The spectra were measured using HA and FA feedstock powders and also the flat monolithic coated substrates to assess the influence of the CoBlast treatment on the HA and FA

crystallinity. The analysis was carried out over the angular range of 20 to 60° (2 $\theta$ ). All XRD scans were carried out with a resolution of 0.04° (2 $\theta$ ) and a sampling time of 3 s per step. Silicon was used as an internal standard to

account for non-linear peak shift. The lattice parameters of the HA and FA powders were calculated using the method of Holland and Redfern and refined using  $d$ -spacings [40].

Surface roughness of the coated titanium coupons was measured using a Taylor-Hobson Pneumo Form Talysurf Series 2 (Leicester, U. K.). Four measurements per each of the five samples were used to determine the average roughness ( $R_a$ ). In order to determine the effect of the process on the titanium substrates, samples were acid etched with 1 M HCl for 90 s in an ultrasonic bath to remove the HA layers; the samples were subsequently ultrasonically cleaned in iso-propanol.

Cross sections of the titanium screws were made in order assess coating thickness and examined using a Leica MEF4M (Wetzlar, Germany) optical microscope with reflected light. To prepare the cross sections for analysis the samples were mounted in a polyester resin, then ground and polished to a 0.04  $\mu\text{m}$  finish, rinsed with water and iso-propanol respectively and dried with a stream of warm air.

#### 2.4 Microstructural characterisation

The microstructure of the metallic substrates was examined using a Leica MEF4M (Wetzlar, Germany) optical microscope. The cross-sections were prepared as described in Sect. 2.3 and etched in Kroll's solution for 15 s to reveal the microstructure [41] and subsequently rinsed thoroughly with water and then isopropanol and dried with a stream of warm air.

#### 2.5 Coating adhesion

A bone model material (Renshape Grade 5460 (Mouldlife, U. K.)) was used to examine the adhesion of the coating to the screws. The model bone was composed of a cured polyurethane resin that mimics the hardness of cortical bone. This material has been used previously to examine the adhesion of coatings to screws [42]. Pilot-holes 3 mm in diameter were drilled into the board and the coated screws were screwed in and out of the holes. The screws were subsequently rinsed with distilled water and iso-propanol to remove debris. Cross-sections of the screws were prepared using the method described in Sect. 2.3. Cross-sections of the screws before and after 'implantation' were examined to ascertain whether there was delamination of the coating during implantation and/or removal. After removal of the screws, the bone model material was sectioned and energy-dispersive X-ray spectroscopy (EDX) analysis was carried out on the model bone material to examine coating loss during insertion, using an Oxford Swift-TM EDX system (Toronto, Canada). All scans were carried out for the same time duration (90 s), at the same magnification ( $\times 1000$ ) at a voltage of 15 kV. EDX is

limited for quantitative surface analysis due to the emission of X-rays from beneath the surface [43], thus here it is used for indicative purposes only.

#### 2.6 Cell culture

MG-63 cells (European Collection of Cell Cultures), a human osteosarcoma cell line derived from a 14 year old male, were maintained in DMEM (Life Technologies) supplemented with 10 % heat inactivated foetal bovine serum (FBS) and 1 % L-glutamine in a humidified atmosphere at 37 °C and 5 % CO<sub>2</sub>. Cells were cultured up to ten passages.

#### 2.7 Cell attachment and morphology

Prior to cell seeding, titanium samples were rinsed in 70 % ethanol followed by sequential washes in sterile water. Samples were then conditioned in complete media. MG-63 cells were seeded at  $4 \times 10^3$  cells per well in 12 well plates with titanium samples. Cells were fixed with 3 % paraformaldehyde (PFA; Sigma Aldrich) at room temperature for 20 min following a 1 or 5 day incubation. Fixed cells were stained with Hoechst 33342 (nuclei; Sigma) and phalloidin-AlexaFluor568 (F-Actin; Life Technologies). Images were acquired with Olympus Scan<sup>R</sup> Automated Image Acquisition Software on a Scan<sup>R</sup> IX81 microscope (Olympus) with an UPLSAPO 20 $\times$  objective (Olympus) and 1344  $\times$  1024 resolution cooled CCD camera. Standard filter sets and 64 subpositions were used. Images were analysed using Columbus image analysis software (Perkin Elmer) to determine nuclear size and roundness and cell number, size and roundness. One-way ANOVA was used for group comparison and a  $P < 0.05$  was deemed to be significant.

### 3 Results

#### 3.1 Surface characterisation

XRD analysis was carried out on the as-received powder and the deposited HA and FA coatings. Figure 3 shows the XRD patterns for HA and FA starting powders. The HA and FA powders exhibited similar diffraction patterns. Examination of (300) reflection shows a shift to a higher angle for the FA compared to the HA, Fig. 4. This is due to a reduction in the  $a$ -axis dimension of the FA compared to the HA. This reduction is due to the presence of the smaller F<sup>-</sup> ions in the FA lattice compared to the larger OH<sup>-</sup> ions in the HA lattice [44]. To confirm there was a reduction in the  $a$ -axis dimension of the FA, the lattice parameters of

**Fig. 3** XRD patterns of the as received HA powder and FA powder, the dashed lines correspond to silicon peaks

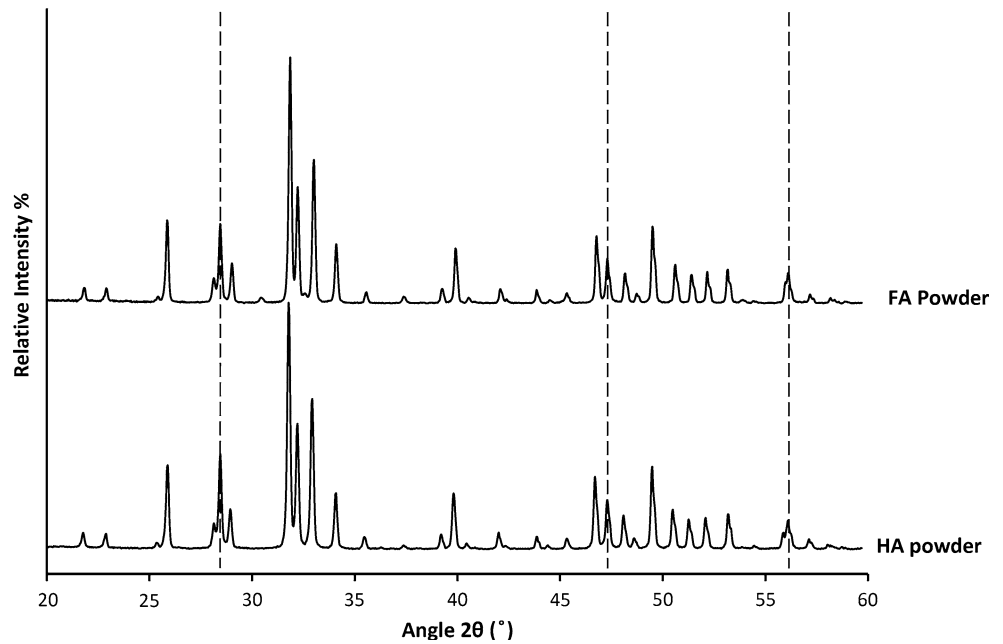


**Fig. 4** Shift of (300) reflection between HA and FA

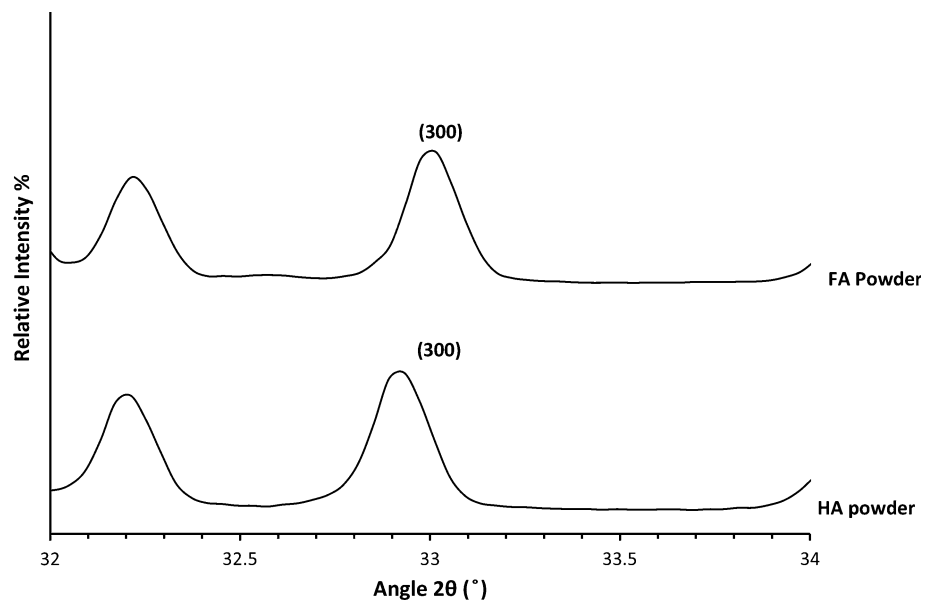


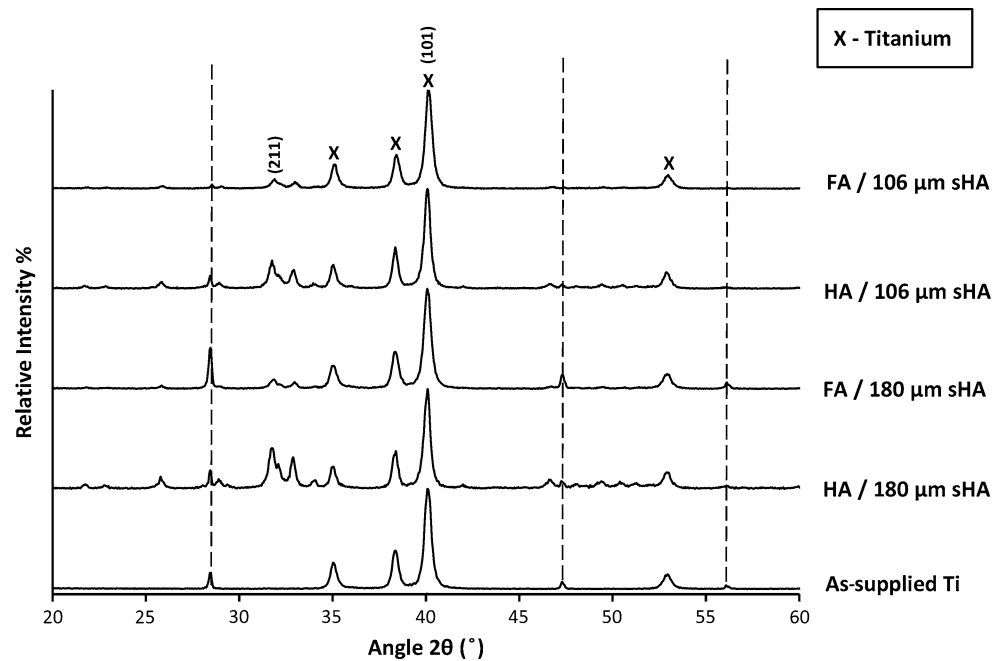
**Table 1** Lattice parameters of as received HA and FA powders

Phase	<i>a</i> (Å)	<i>c</i> (Å)
HA powder	9.4180	6.8831
FA powder	9.4037	6.8889

both powders were calculated as described in Sect. 2.3. The computed lattice parameters showed a reduction in the *a*-axis dimension for the FA compared to the HA. The computed lattice parameters for both the HA and FA powder are shown in Table 1.

Figure 5 shows XRD plots of the as-supplied titanium and the coated substrates. The coated substrates did not exhibit any additional peaks associated with  $\alpha/\beta$ -TCP or an amorphous halo in the 30–35° ( $2\theta$ ) region. This indicates that there was minimal change to the precursor HA and FA powders during processing. This is as expected due to the low temperature (<50 °C) nature of the process. The samples exhibited peaks associated with titanium which are present due to the underlying titanium substrate due to the very thin HA and FA layers deposited (<5  $\mu\text{m}$ ). The samples coated with HA exhibited a stronger trace of the coating compared to the sample coated with FA. The ratio

**Fig. 5** XRD patterns of the as-supplied titanium coupons, HA/180, FA/180, HA/106 and FA/106  $\mu\text{m}$  sHA prepared surfaces. The dashed lines correspond to silicon peaks. The titanium peaks are marked with an X while all other peaks correspond to HA and FA respectively



of the most intense HA peak, at the (211) plane, to the most intense Ti peak, at the (101) plane, was 0.37 and 0.28 for the HA/180 and HA/106  $\mu\text{m}$  sHA, respectively while the ratio of the most intense FA peak, at the (211) plane, to the most intense Ti peak, at the (101) plane, was 0.10 and 0.09 for the HA/180 and HA/106  $\mu\text{m}$  sHA, respectively. This is due to a thicker coating of HA compared to FA.

The surface topography was examined using contact profilometry and SEM analysis. The average surface roughness and the roughness profile along the surface of the samples after the surface modification is shown in Fig. 6. The average surface roughness ( $R_a$ ) of each of the samples increased after surface modification compared to the unmodified titanium. One-way analysis of variance (ANOVA) was performed to determine whether the difference in roughness between the various substrates was statistically significant. A  $P$  value  $< 0.05$  was deemed to be significant. The test yielded a  $P$  value =  $1.5 \times 10^{-28}$ . This indicates that the roughness was significantly influenced by the type of blast medium used. A Tukey post hoc test was performed to determine which surfaces had statistically significant different roughness. The results are shown in Table 2. The surface roughness of the as-supplied titanium yielded a  $P$  value  $< 0.05$  when compared to each of the coated surfaces indicating that the blasting process significantly alters the surface roughness.

The particle size also affected the surface roughness as substrates blasted with the larger 180  $\mu\text{m}$  sHA gave rise to a significantly rougher surface than substrates blasted with the 106  $\mu\text{m}$  sHA particle. The 106 sHA increased the roughness by a factor of 3.8 while the 180 sHA increased the surface roughness by a factor of 6.3.

The test was also used to assess the influence of the blast media on the underlying substrate in isolation by measuring the surface roughness after removal of the coating via an acid etch. The roughness of the underlying titanium is important to allow for mechanical interlock between the implant and the host tissue after resorption of the HA [45]. Comparison of the coated and etched substrates blasted with the same blast medium and coating medium yielded  $P$  values  $> 0.05$ , indicating no statistical significance in the roughness of the coated and etched samples.

Figure 7 shows the results of SEM imaging of the surface of the as-supplied titanium and the surfaces of the treated substrates before and after removal of the coating via the acid etch. The substrates exhibit a variety of features after acid etching: there are clear tears, scratches, and ridges evident. These features are more evident on the coupons blasted with the 180  $\mu\text{m}$  sHA than the 106  $\mu\text{m}$  sHA due to the greater abrasion of the larger particle.

Cross-sections of the as-received dental screws and the coated screws are shown in Fig. 8. The figure highlights the thin coating ( $< 5 \mu\text{m}$ ) of HA and FA produced by the CoBlast process. The threads of the CoBlasted screws exhibited rounding compared to the unmodified screw. This is due to the abrasive nature of the CoBlast process. The degree of rounding was more significant for the screws blasted with the 180  $\mu\text{m}$  sHA than the 106  $\mu\text{m}$  sHA. Figure 9 shows SEM images of the coatings on the surface of the screws. The coating thickness varied depending on the type of blast media and coating particle used. The average coating thickness of the HA/106, HA/180, FA/106, FA/180  $\mu\text{m}$  sHA coating were 4.9, 6.3, 2.4 and 2.8  $\mu\text{m}$

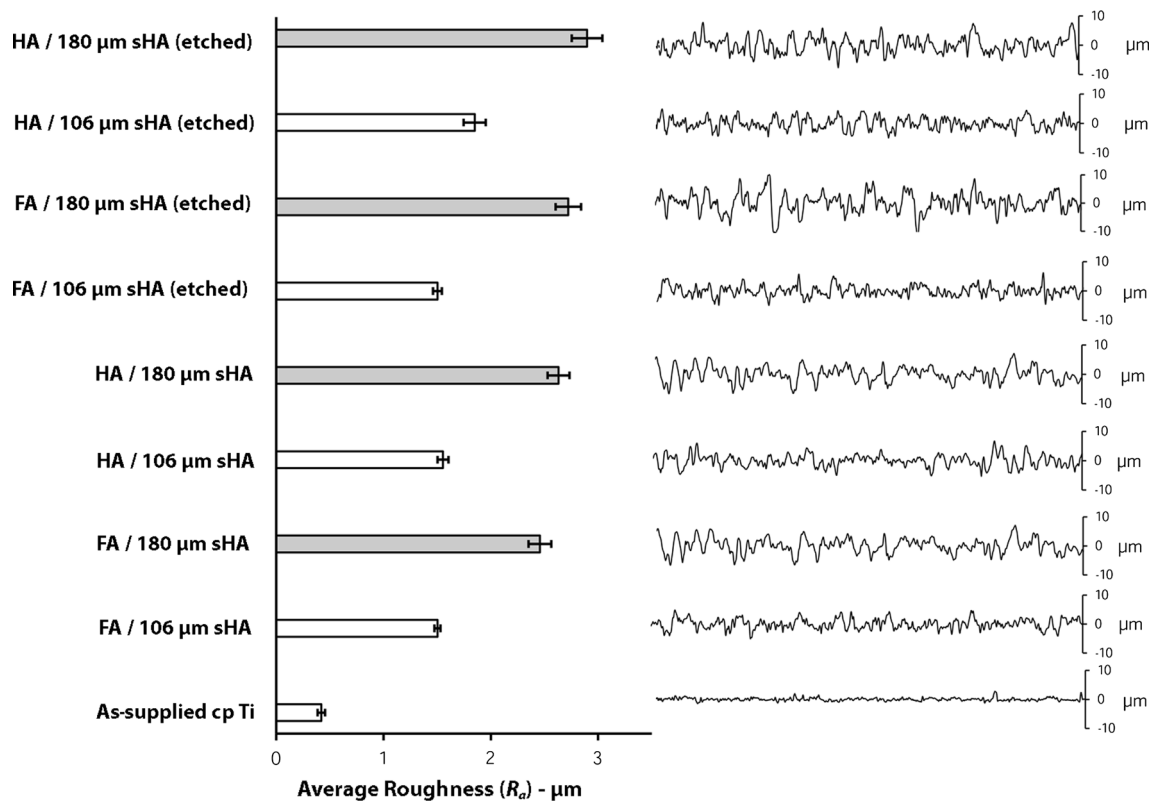


**Fig. 6** The average surface roughness and the roughness profile (5 mm) along the surface of the samples after the surface modification. Error bars indicate standard deviation

**Table 2** *P*-values from post hoc Tukey test of the substrate surface roughness

		<i>P</i> value
As-supplied Ti	FA 106	0.000
As-supplied Ti	FA 180	0.000
As-supplied Ti	HA 106	0.000
As-supplied Ti	HA 180	0.000
As-supplied Ti	FA 106 (etched)	0.000
As-supplied Ti	FA 180 (etched)	0.000
As-supplied Ti	HA 106 (etched)	0.000
As-supplied Ti	HA 180 (etched)	0.000
FA 106	FA 180	0.000
HA 106	HA 180	0.000
FA 106	FA 106 (etched)	0.898
FA 180	FA 180 (etched)	0.055
HA 106	HA 106 (etched)	0.054
HA 180	HA 180 (etched)	0.346

respectively. The difference coating thickness between the HA and the FA coatings may be due to the difference in the particle size of the powders used. The HA a particle size of 25–60 μm and the FA had a particle size of 5–30 μm.

### 3.2 Coating adhesion

Figure 10 shows the coated screws that were not inserted into the model bone (left) and screws after insertion into and subsequent removal from the model bone (right). From the optical micrographs the coating did not exhibit signs of delamination. The screws after insertion retain similar feature to the un-inserted screws. It should be noted that there is an apparent difference in screw width between the un-inserted FA/180 μm screw and the FA/180 μm screw after insertion into the model bone. This is due to the depth of grinding of the screw during the preparation of a cross section for optical microscopy. EDX analysis of the model bone material after removal of the screw yielded no elements from the uncoated screw while trace amounts of calcium only were detected on all of the model bone material that had coated screws inserted.

### 3.3 Microstructural characterisation

The microstructures of the dental screws were examined to assess what influence the coating process had on the screws' microstructure. As shown in Fig. 11, the screws treated via the CoBlast process exhibit a change in their microstructure compared to the as supplied cp-titanium

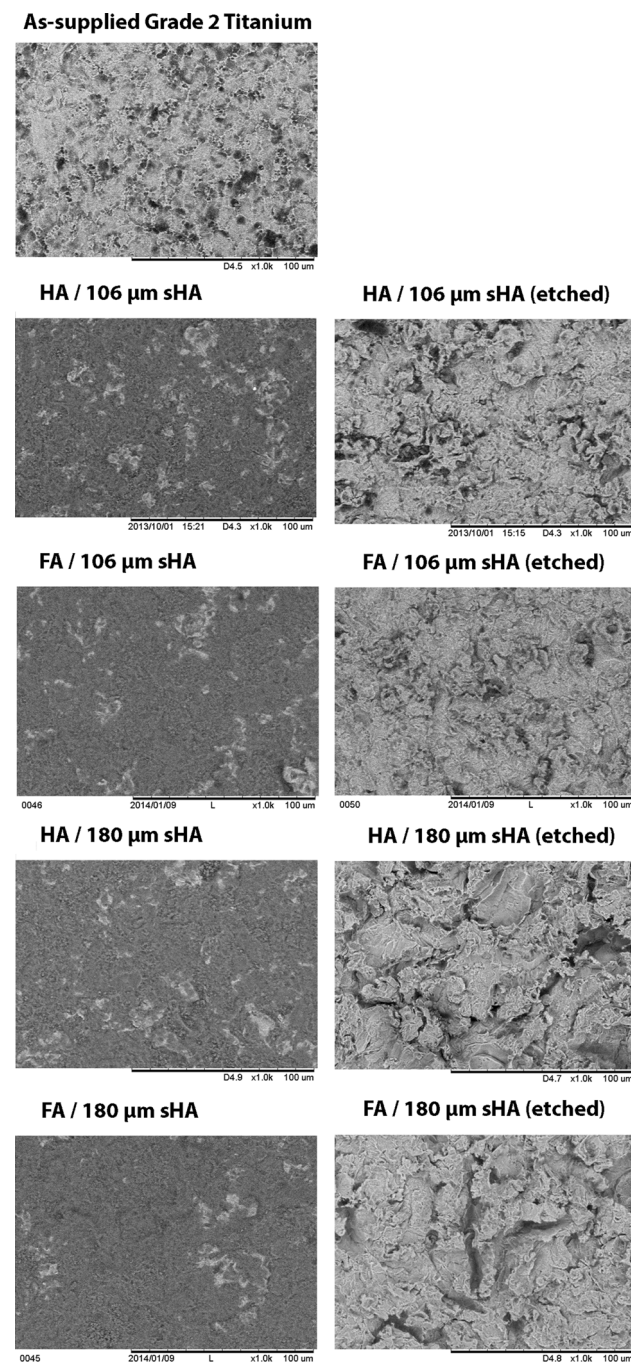


**Fig. 7** SEM images of the surface of as received titanium coupon and the coated samples before and after removal of the coating via an acid etch

screws. Three different regions were observed in the in the substrates treated using this process, a severely deformed surface layer, a region characterised by gross deformation of the grains and the un-deformed substrate consisting of equiaxed  $\alpha$ -grains. These three different regions have previously been identified by Jiang et al. for sandblasted cp-titanium [46]. The region characterised by gross deformation of the grains exhibited twinning.

### 3.4 Cell attachment and morphology

In order to assess cell attachment and cell morphology MG-63 cells were cultured on the various surfaces followed by fixation, staining and analysis using a high content automated imaging and analysis platform. The cell attachment and cell morphology results are shown in Fig. 12. Cell attachment was measured as cell counts and cell morphology determined as nuclear size, nuclear roundness, cell size and cell roundness.

Since the surfaces of the samples are uneven it is not possible to focus on all cells within a single field of view. This limitation affected cell segmentation during image analysis and meant accurate cell number comparisons between rough and smooth surfaces could not be determined, hence only the results for the rough surface (HA/180  $\mu$ m sHA (etched), HA/180  $\mu$ m sHA and HA/180  $\mu$ m sHA) are presented. This was deemed valid as previous studies have shown that roughened surfaces enhance cellular attachment, proliferation and differentiation compared to smooth surfaces [10–12]. Examining the cell numbers after 1 and 5 days there was no statistical difference ( $P_{1 \text{ day}} < 0.54$ ,  $P_{5 \text{ days}} < 0.06$ ) between roughened titanium sample (HA/sHA (etched) and the CoBlasted surfaces which contained a rough bioactive surface. Additionally there were no statistical significances for cell morphological measurements between the different surfaces ( $P_{1 \text{ day}} < 0.31$ ,  $P_{5 \text{ days}} < 0.07$ ). The cells seeded on each surface exhibited similar morphology at 1 and 5 days. Figure 12 shows the cells seeded onto the various surfaces after 5 days.

## 4 Discussion

CoBlast is a novel coating technique that has been used in previous studies to deposit hydroxyapatite onto various metallic substrate types [29–35]. In these previous studies the HA was deposited onto flat coupons. This study investigates the disposition HA and FA using this novel coating technique onto more complex geometrical shapes (dental screws).

The optical micrographs of the titanium screws after the deposition process exhibit a coating  $<5 \mu$ m thick on the surface of the screws. Previous studies have shown that altering the abrasive to dopant ratio, powder chemistry, blast pressure and blast height can alter the coating thickness marginally, but coatings in excess of 10 microns are rare and are not likely with the materials described herein [29–35]. The coating thickness is independent of spraying time, as the process gives a balance of abrasion and deposition. Additional spraying merely produces additional substrate erosion, but the coating thickness does not change significantly.



**Fig. 8** Optical micrographs of the as received dental screws and the coated screws. The black layer represents the HA and FA coatings

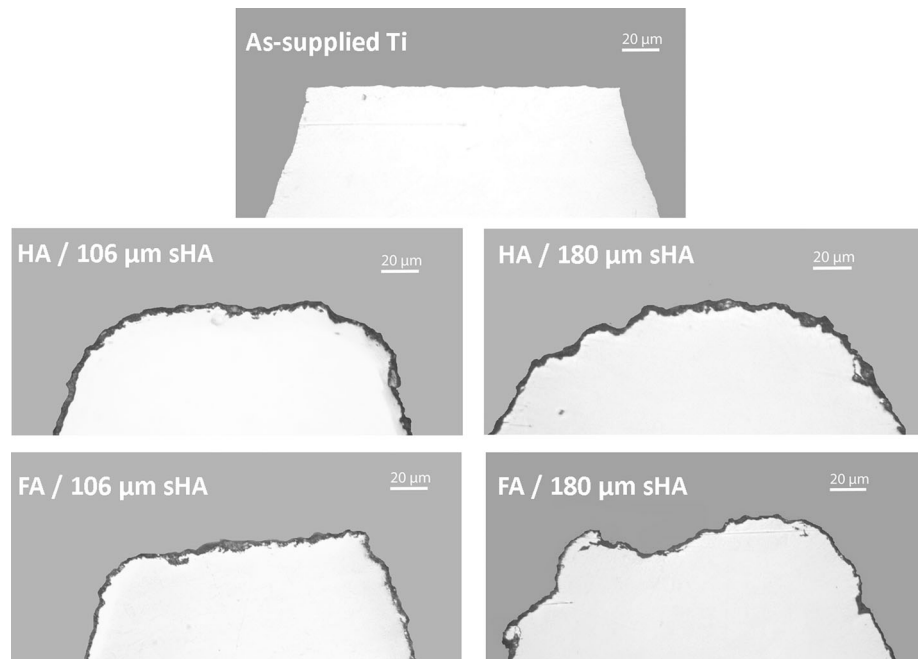
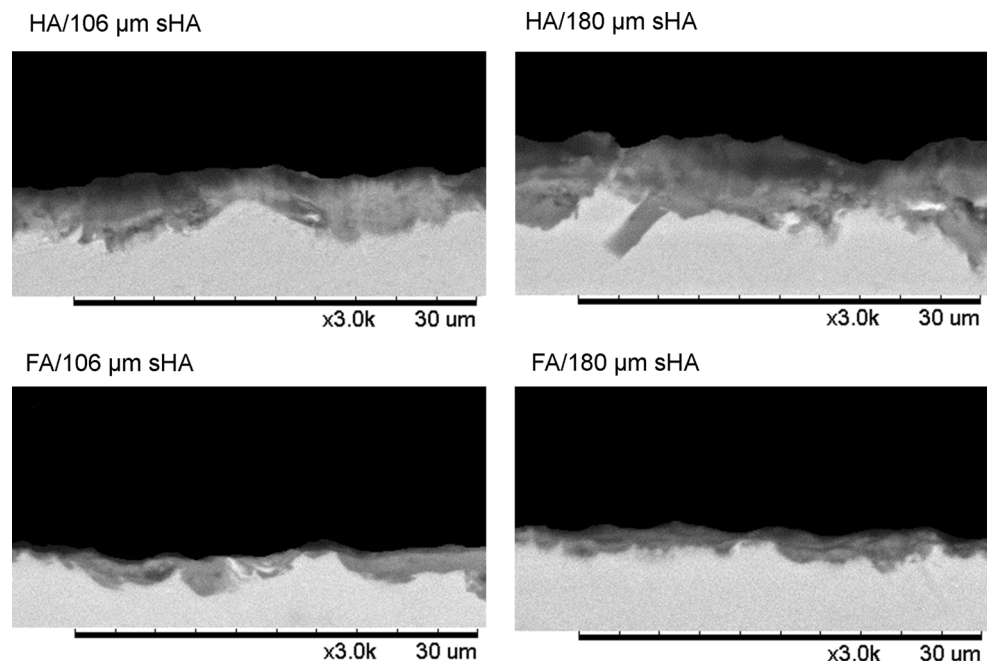


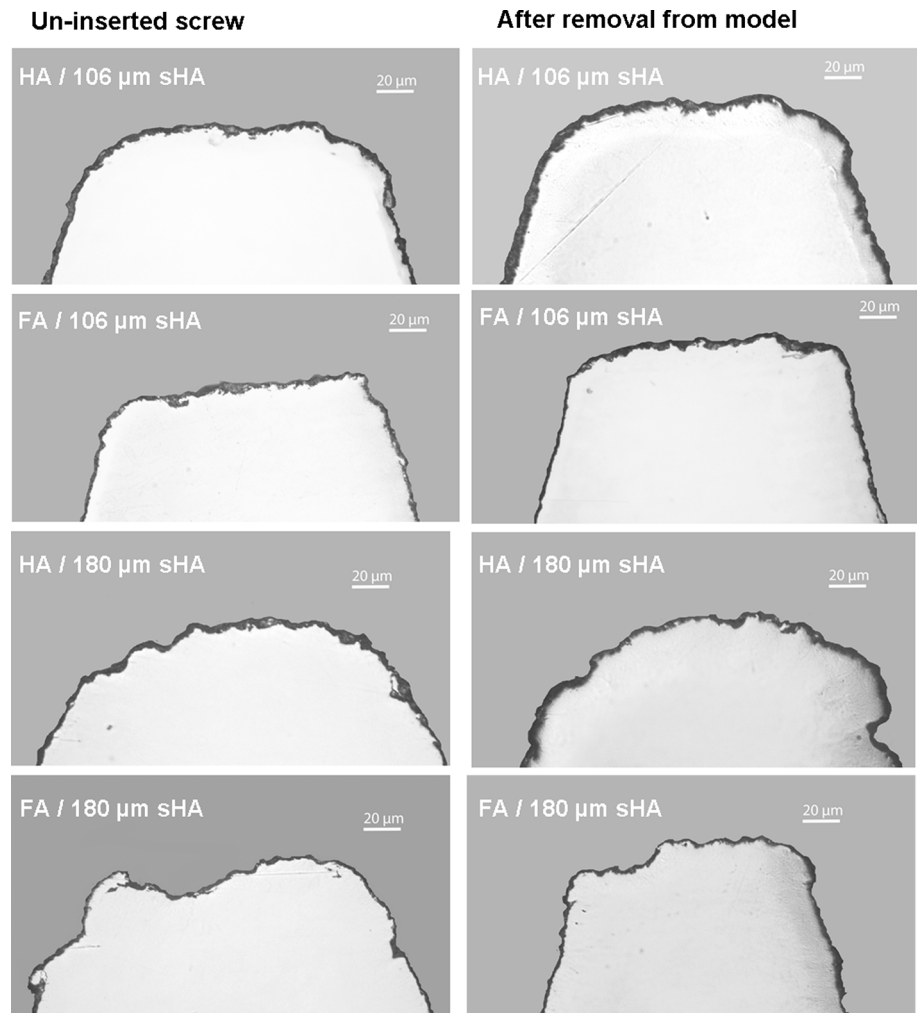
**Fig. 9** Cross-section SEM images of the coatings on the surface of the screws



Comparing the coated screws with the unmodified screw, there is a change in screw morphology. The threads of the coated screws exhibit rounding; this is due to the abrasive nature of the coating process. The degree of abrasion and rounding of the screw threads was dependent on the size of the blast medium particle used. The screws blasted with the 106 μm sHA broadly retained the trapezoidal shape of the screw with minimal rounding of the threads. The screws blasted using the 180 μm sHA

particles exhibited significantly greater abrasion and rounding. This is due to the larger particle size of the 180 μm sHA particle. Although, the change in screw morphology is undesirable, previous studies suggest this does not adversely affect bone formation around the screw. Previous studies have reported grit blasted screws to exhibit a higher bone-to-metal contact than as-machined screws and require more torque to remove them from bone [13–15].

**Fig. 10** Optical micrographs of dental screws coated with HA and FA. Un-inserted screws (*left*) and screws after insertion into and subsequent removal from the model bone (*right*). The inserted screws do not show signs of delamination of the coating



Examining the surface roughness ( $R_a$ ) of the coupons, Fig. 6, the 180  $\mu\text{m}$  sHA particles significantly increase the surface roughness compared to the coupons blasted with the 106  $\mu\text{m}$  sHA particles. SEM images of the etched coupons show that the coupons blasted with the 180  $\mu\text{m}$  sHA particles had deeper and wider tears and scratches than the coupons blasted with 106  $\mu\text{m}$  sHA particles, Fig. 7. Although, there is a significant difference in the roughness of the coupons blasted with the 106 and 180  $\mu\text{m}$  sHA, both have roughness within the reported optimum range for osteointegration (1–10  $\mu\text{m}$ ) [3].

The assessment of the coating adhesion via insertion the screws into a model bone material provides a good assessment of how the coating will respond to biomechanical forces in clinical applications [47]. EDX scans of the bone model material after removal of the unmodified screw did not detect the presence of any elements. This indicates that there was no wear or fretting of the titanium during insertion. For the model bone inserted with coated screws, trace amount of calcium only were detected. This

calcium is due to HA and FA particles liberated during insertion. It should be noted that calcium signal was very weak and that no phosphorous was detected indicating that the coating loss was minimal. As discussed in Sect. 2.5, EDX is limited for quantitative analysis surface analysis and thus was used here for indicative purposes only. Further, analysis is required to quantify the degree of wear and fretting of the titanium and coating loss during insertion of the screws. Examining the cross-sections of the screws before and after removal from the model bone, Fig. 10, there appears to be no obvious signs of damage to the coating indicating that there was minimal coating loss during to insertion of the screws.

The CoBlast process resulted in a change in the screws microstructure compared to the unmodified screws, coated screws exhibit a severely deformed surface layer, a region characterised by gross deformation of the grains and an undeformed substrate consisting of equiaxed  $\alpha$ -grains, within the region characterised by gross deformation of the grains twinning was observed. Twinning has previously been

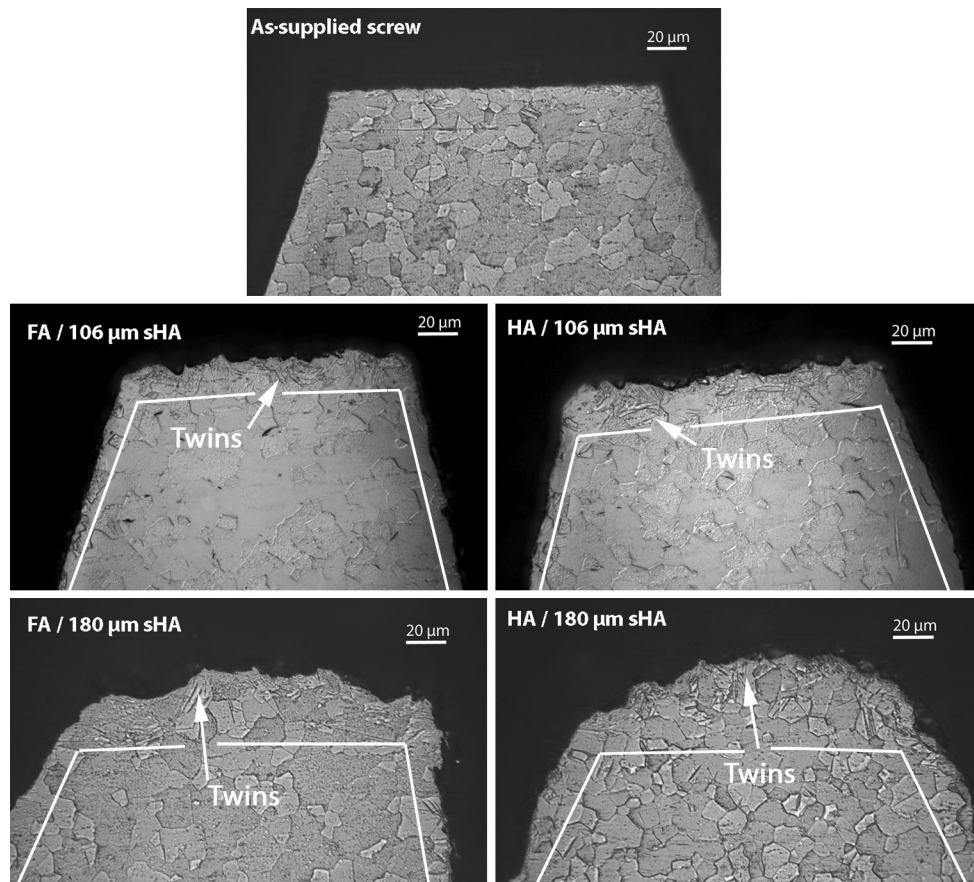


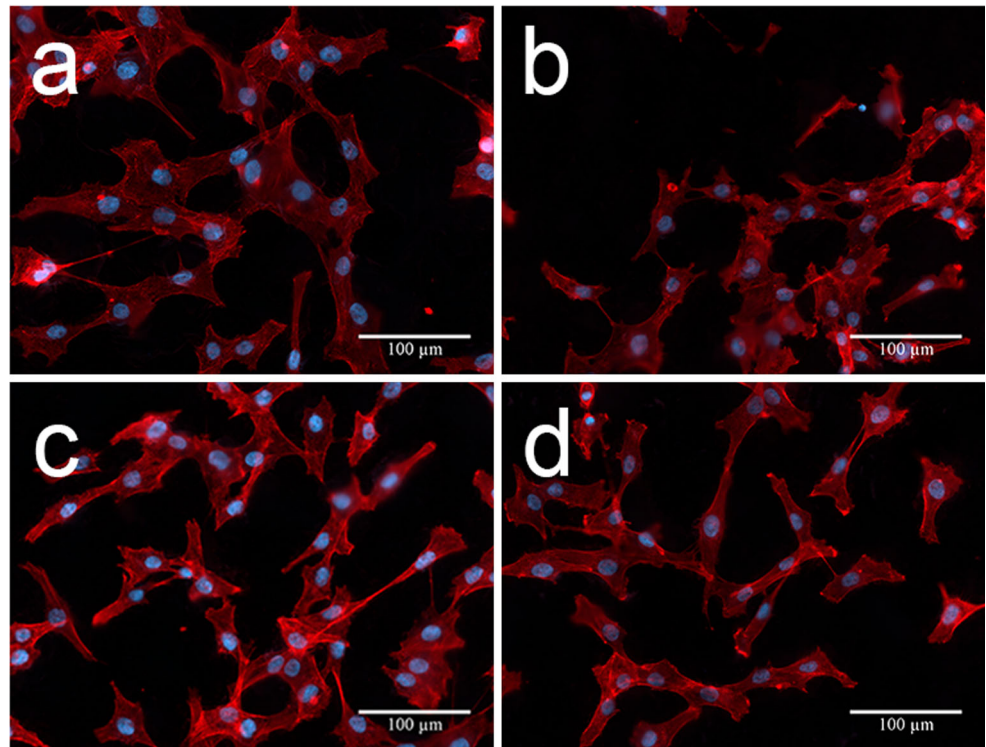
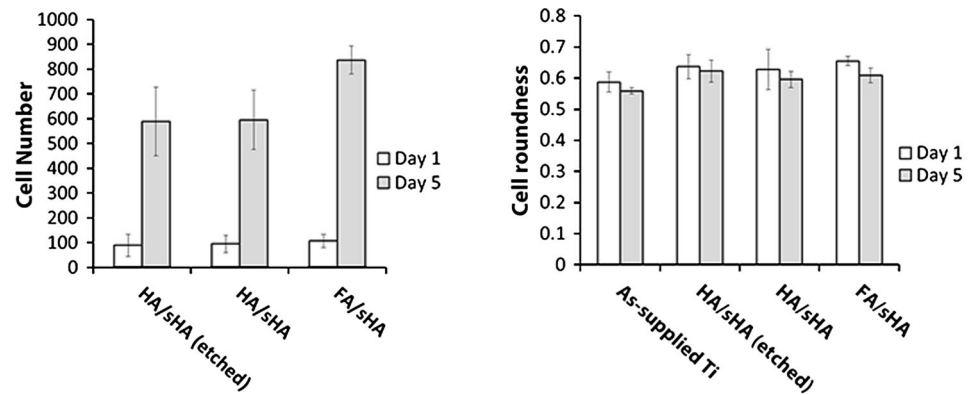
**Fig. 11** Etched cross-sections of titanium screws (As supplied titanium screw, FA/106, HA/106, FA/180 and HA/180 sHA, respectively). The treated screws exhibit signs of plastic deformation and twin formation. The white line outlines this deformation zone

observed in shot peened cp-titanium [48]. The formation of twins is promoted by a high strain rate, shock loading and relatively large grain size [49]. This deformation and twinning is most pronounced at sites normal to the blast stream, such as the tip of the screw threads. This is due to the orientation of the screw to the blast stream. The tip of the threads are normal to the blast stream, thus a higher percentage of the particle energy is imparted to the surface compared to the sides of the threads [50]. For the screws blasted with the 180  $\mu\text{m}$  sHA, the change in microstructure was identified to a depth of 30  $\mu\text{m}$  from the surface of the tip of the thread while at the sides of the thread the change in microstructure was to a depth of 10  $\mu\text{m}$ . The screws blasted with 106  $\mu\text{m}$  sHA exhibited a change in microstructure to a depth of 20  $\mu\text{m}$  from the surface of the tip of the thread while at the sides of the thread the change in microstructure was to a depth of 5  $\mu\text{m}$ . The formation of the severely deformed surface layer may be beneficial as the associated compressive strength in the surface layer improves fatigue performance, a key material property for medical device implants [46, 51].

The *in vitro* tests indicate that there is no statistical difference in cell numbers at 1 and 5 days between the roughened titanium sample (HA/sHA (etched) and the CoBlasted surfaces which contained a rough bioactive surface (HA/sHA and FA/sHA). Previous studies have shown that rough surfaces enhance cell attachment, proliferation and differentiation compared to smooth surfaces [10–12]. This indicates that this coating process can incorporate a bioactive coating onto a roughened surface without adversely affecting the initial cell response. Similarly, there was no statistical difference in the nuclear or cell morphologies between the cells seeded onto the blanks and the cells seeded onto the other surfaces; this would indicate that the process does not adversely affect cell health.

It should be highlighted that *in vitro* models are simplistic models that do not account for the complex biological interactions within biological systems and that further *in vivo* testing is required to fully assess the biological response to bioactive coatings deposited using this process.

**Fig. 12** Cell numbers (*left*) and cell roundness (*right*) on the prepared surfaces after 1 and 5 days. *Error bars* indicate standard deviation. Images of the cells seeded onto the various surface types ( $\times 20$  magnification), **a** Blank, **b** HA/sHA etched, **c** HA/sHA and **d** FA/sHA (after 5 days/s). Cell nuclei are stained with Hoechst 33342 (*blue*) and cell boundaries (F-actin) are visualised with phalloidin-AlexaFluor568 (*red*) (Color figure online)



## 5 Conclusions

The CoBlast process can be used to deposit highly adherent coatings of HA and FA onto dental screws. The process alters the morphology of the screw threads the degree of alteration is significantly influenced by the size blast media used. Previous studies indicate that moderate alteration of the screws morphology does this does not adversely affect performance *in vivo*. Initial *in vitro* tests on substrates coated using this process indicate that it does not adversely affect the biological response of cells.

**Acknowledgments** The authors wish to thank the Programme for Research in Third Level Institutions (PRTL) for part funding of the project and EnBio Ltd. for providing the materials to undertake the study. The UCD Cell Screening Lab acknowledges financial support from the UCD College of Science.

## References

- Schuh A, Bigoney J, Hönlle W, Zeiler G, Holzwarth U, Forst R. Second generation (low modulus) titanium alloys in total hip arthroplasty. *Mater Werkst.* 2007;38(12):1003–7.
- Cho SA, Park KT. The removal torque of titanium screw inserted in rabbit tibia treated by dual acid etching. *Biomaterials.* 2003;24(20):3611–7.
- Le Guéhennec L, Soueidan A, Layrolle P, Amouriq Y. Surface treatments of titanium dental implants for rapid osseointegration. *Dent Mater.* 2007;23(7):844–54.
- Albrektsson T, Johansson C. Osteoinduction, osteoconduction and osseointegration. *Eur Spine J.* 2001;10(2):S96–101.
- Ellingsen JE. Surface configurations of dental implants. *Periodontology* 2000. 1998;17(1):36–46.
- Sul YT, Kang BS, Johansson C, Um HS, Park CJ, Albrektsson T. The roles of surface chemistry and topography in the strength and rate of osseointegration of titanium implants in bone. *J Biomed Mater Res Part A.* 2009;89A(4):942–50.

7. Buser D, Schenk RK, Steinemann S, Fiorellini JP, Fox CH, Stich H. Influence of surface characteristics on bone integration of titanium implants. A histomorphometric study in miniature pigs. *J Biomed Mater Res.* 1991;25(7):889–902.
8. Larsson C, Thomsen P, Aronsson BO, Rodahl M, Lausmaa J, Kasemo B, Ericson LE. Bone response to surface-modified titanium implants: studies on the early tissue response to machined and electropolished implants with different oxide thicknesses. *Biomaterials.* 1996;17(6):605–16.
9. Suzuki K, Aoki K, Ohya K. Effects of surface roughness of titanium implants on bone remodeling activity of femur in rabbits. *Bone.* 1997;21(6):507–14.
10. Bowers KT, Keller JC, Randolph BA, Wick DG, Michaels CM. Optimization of surface micromorphology for enhanced osteoblast responses in vitro. *Int J Oral Maxillofac Implant.* 1991;7(3):302.
11. Martin J, Schwartz Z, Hummert T, Schraub D, Simpson J, Lankford J, Dean D, Cochran D, Boyan B. Effect of titanium surface roughness on proliferation, differentiation, and protein synthesis of human osteoblast-like cells (MG63). *J Biomed Mater Res.* 1995;29(3):389–401.
12. Lincks J, Boyan BD, Blanchard CR, Lohmann CH, Liu Y, Cochran DL, Dean DD, Schwartz Z. Response of MG63 osteoblast-like cells to titanium and titanium alloy is dependent on surface roughness and composition. *Biomaterials.* 1998;19(23):2219–32.
13. Wennerberg A, Albrektsson T, Johansson C, Andersson B. Experimental study of turned and grit-blasted screw-shaped implants with special emphasis on effects of blasting material and surface topography. *Biomaterials.* 1996;17(1):15–22.
14. Wennerberg A, Albrektsson T, Andersson B, Krol JJ. A histomorphometric study of screw-shaped and removal torque titanium implants with three different surface topographies. *Clin Oral Implant Res.* 1995;6(1):24–30.
15. Wennerberg A, Ektessabi A, Albrektsson T, Johansson C, Andersson B. A 1-year follow-up of implants of differing surface roughness placed in rabbit bone. *Int J Oral Maxillofac Implant.* 1996;12(4):486–94.
16. Schwartz Z, Raz P, Zhao G, Barak Y, Tauber M, Yao H, Boyan BD. Effect of micrometer-scale roughness of the surface of Ti6Al4V pedicle screws in vitro and in vivo. *J Bone Joint Surg.* 2008;90(11):2485–98.
17. Klokkevold PR, Nishimura RD, Adachi M, Caputo A. Osseointegration enhanced by chemical etching of the titanium surface. A torque removal study in the rabbit. *Clin Oral Implant Res.* 1997;8(6):442–7.
18. Blokhuis TJ, Arts JJC. Bioactive and osteoinductive bone graft substitutes: definitions, facts and myths. *Injury.* 2011;42:S26–9.
19. Haverty D, Tofail SAM, Stanton KT, McMonagle JB. Structure and stability of hydroxyapatite: density functional calculation and Rietveld analysis. *Phys Rev B.* 2005;71(9):094103.
20. Tofail SAM, Haverty D, Stanton KT, McMonagle JB. Structural order and dielectric behaviour of hydroxyapatite. *Ferroelectrics.* 2005;319(1):117–23.
21. Hench LL. Bioceramics: from concept to clinic. *J Am Ceram Soc.* 1991;74(7):1487–510.
22. Bloebaum RD, Beeks D, Dorr LD, Savory CG, Dupont JA, Hofmann AA. Complications with hydroxyapatite participate separation in total hip arthroplasty. *Clin Orthop Relat Res.* 1994;298:19–26.
23. Collier JP, Surprenant VA, Mayor MB, Wrona M, Jensen RE, Surprenant HP. Loss of hydroxyapatite coating on retrieved, total hip components. *J Arthroplast.* 1993;8(4):389–93.
24. Hardy DR, Frayssinet P, Bonel G, Authom T, Naelou SAL, Delincé PE. Two-year outcome of hydroxyapatite-coated prostheses: two femoral prostheses retrieved at autopsy. *Acta Orthop.* 1994;65(3):253–7.
25. Lintner F, Bohm G, Huber M, Scholz R. Histology of tissue adjacent to an HAC-coated femoral prosthesis. A case report. *J Bone Jt Surg Br Vol.* 1994;76-B(5):824–830.
26. Morscher E. Hydroxyapatite coating of prostheses. *J Bone Jt Surg Br Vol.* 1991;73-B(5):705–706.
27. O'Flynn K, Stanton K. Optimisation of the enamelling of an apatite–mullite glass–ceramic coating on Ti6Al4V. *J Mater Sci Mater Med.* 2011;22(9):2035–44.
28. Overgaard S, Lind M, Josephsen K, Maunsbach AB, Bünger C, Søballe K. Resorption of hydroxyapatite and fluorapatite ceramic coatings on weight-bearing implants: a quantitative and morphological study in dogs. *J Biomed Mater Res.* 1998;39(1):141–52.
29. O'Neill L, O'Sullivan C, O'Hare P, Sexton L, Keady F, O'Donoghue J. Deposition of substituted apatites onto titanium surfaces using a novel blasting process. *Surf Coat Technol.* 2009;204(4):484–8.
30. Dunne CF, Twomey B, O'Neill L, Stanton KT. Co-blasting of titanium surfaces with an abrasive and hydroxyapatite to produce bioactive coatings: substrate and coating characterisation. *J Biomater Appl.* 2013;28(5):767–78.
31. Barry JN, Twomey B, Cowley A, O'Neill L, McNally PJ, Dowling DP. Evaluation and comparison of hydroxyapatite coatings deposited using both thermal and non-thermal techniques. *Surf Coat Technol.* 2013;226:82–91.
32. O'Hare P, Meenan BJ, Burke GA, Byrne G, Dowling D, Hunt JA. Biological responses to hydroxyapatite surfaces deposited via a co-incident microblasting technique. *Biomaterials.* 2010;31(3):515–22.
33. O'Sullivan C, O'Hare P, Byrne G, O'Neill L, Ryan KB, Crean AM. A modified surface on titanium deposited by a blasting process. *Coatings.* 2011;1(1):53–71.
34. O'Sullivan C, O'Hare P, O'Leary ND, Crean AM, Ryan K, Dobson ADW, O'Neill L. Deposition of substituted apatites with anticolonizing properties onto titanium surfaces using a novel blasting process. *J Biomed Mater Res B Appl Biomater.* 2010;95(1):141–9.
35. Byrne GD, O'Neill L, Twomey B, Dowling DP. Comparison between shot peening and abrasive blasting processes as deposition methods for hydroxyapatite coatings onto a titanium alloy. *Surf Coat Technol.* 2013;216:224–31.
36. Prevy P. X-ray diffraction characterization of crystallinity and phase composition in plasma-sprayed hydroxyapatite coatings. *J Therm Spray Technol.* 2000;9(3):369–76.
37. Tsui YC, Doyle C, Clyne TW. Plasma sprayed hydroxyapatite coatings on titanium substrates Part 1: mechanical properties and residual stress levels. *Biomaterials.* 1998;19(22):2015–29.
38. Sobieszczyk S, Zieliński A. Coatings in arthroplasty: review paper. *Adv Mater Sci.* 2008;8(4):35–54.
39. Cook SD, Thomas KA, Kay JF. Experimental coating defects in hydroxylapatite-coated implants. *Clin Orthop Relat Res.* 1991;265:280–90.
40. Holland TJB, Redfern SAT. Unit cell refinement from powder diffraction data; the use of regression diagnostics. *Miner Mag.* 1997;61(1):65–77.
41. Gammon LM, Briggs RD, Packard JM, Batson KW, Boyer R, Dombay CW. Metallography and microstructures of titanium and its alloys. *Materials Park: ASM International, Member/Customer Service Center;* 2004
42. Linderbäck P, Areva S, Aspenberg P, Tengvall P. Sol–gel derived titania coating with immobilized bisphosphonate enhances screw fixation in rat tibia. *J Biomed Mater Res, Part A.* 2010;94(2):389–95.
43. Goodhew PJ, Humphreys FJ, Beanland R. *Electron microscopy and analysis.* London: Taylor & Francis; 2001.
44. Okazaki M, Hirata I, Matsumoto T, Takahashi J. Advantages of TOF-SIMS analysis of hydroxyapatite and fluorapatite in comparison with XRD, HR-TEM and FT-IR. *Dent Mater J.* 2005;24(4):508.

45. Epinette JA, Manley MT. Fifteen years of clinical experience with hydroxyapatite coating in joint arthroplasty. France: Springer; 2004.
46. Jiang XP, Wang XY, Li JX, Li DY, Man CS, Shepard MJ, Zhai T. Enhancement of fatigue and corrosion properties of pure Ti by sandblasting. *Mater Sci Eng, A*. 2006;429(1–2):30–5.
47. Lilja M, Sørensen JH, Sørensen TC, Åstrand M, Procter P, Steckel H, Strømme M. Impact of Biomechanical Forces on Antibiotics Release Kinetics from Hydroxyapatite Coated Surgical Fixation Pins. *J Biomater Nanobiotechnol*. 2013;4:343–50.
48. Thomas M, Lindley T, Jackson M. The microstructural response of a peened near- $\alpha$  titanium alloy to thermal exposure. *Scripta Mater*. 2009;60(2):108–11.
49. Christian JW, Mahajan S. Deformation twinning. *Prog Mater Sci*. 1995;39(1–2):1–157.
50. Momber A. Blast cleaning technology. Heidelberg: Springer; 2008.
51. Teoh SH. Fatigue of biomaterials: a review. *Int J Fatigue*. 2000;22(10):825–37.